Two-body photodisintegration of ^{3}He and ^{3}H†

B. F. Gibson
Los Alamos Scientific Laboratory, Los Alamos, New Mexico 87544

D. R. Lehman
Department of Physics, The George Washington University, Washington, D. C. 20006

(Received 19 August 1974)

Cross sections for two-body photodisintegration of ^{3}He and ^{3}H are calculated in electric-dipole approximation. The calculation is performed within the context of exact three-body theory with the two-nucleon interactions represented by s-wave spin-dependent separable potentials fitted to the low-energy nucleon-nucleon scattering data. The two-body photodisintegration amplitude is expressed in terms of the half-off-shell nucleon plus correlated-pair amplitudes, a method applicable to any weak-process disintegration amplitude. The numerical results indicate: (1) The ^{3}He and ^{3}H 90° photodisintegration cross sections are essentially identical in shape, being only slightly displaced at low energy due to the different thresholds, when both initial and final states are treated consistently. (2) The ^{3}He$(\gamma, d)p$ 90° differential cross section has a peak value of approximately 95 μb/sr.

[NUCLEAR REACTIONS Photodisintegration of ^{3}He and ^{3}H; exact three-body calculation; separable potentials; charge-dependent interactions.]

I. INTRODUCTION

The work of Barbour and Phillips on the low-energy ($E_\gamma \lesssim 40$ MeV) two- and three-body photodisintegration of ^{3}He, delineates the important physical aspects of these processes.[1] For two-body photodisintegration, their exact three-body calculation, which has as input separable, s-wave spin-dependent charge-independent interactions fitted to the two-nucleon effective-range parameters, demonstrates the importance of treating the continuum p-d final state exactly. Compared to neglecting the p-d rescattering, the exact result predicts a peak value for the total cross section ~25% larger. They also find that the spatially mixed-symmetric S component, simulated short-range correlations, and changes in shape and asymptotic form of the spatially symmetric S component (all in the ground state) cause variations in the total cross section of 10% or less; therefore, within the precision of present experiments they can be considered unimportant. The essential picture of the two-body photodisintegration of ^{3}He below $E_\gamma = 40$ MeV is that of an electric-dipole transition from the dominant, spatially symmetric component of the ground state to a p-wave proton-deuteron final state.

Within the above framework, Barbour and Phillips point out an apparent discrepancy between the sets of two-body photodisintegration data available up to 1969. They postulate a ^{3}He ground-state wave function having the analytical form of one obtained from a separable-potential model; however, the binding-energy parameter is set to the experimental value and the spectator function is represented by a double-pole form with one free parameter. The free parameter is determined by fitting the ^{3}He charge radius, this being assumed to be the relevant physical quantity due to the emphasis placed on the asymptotic region by the electric-dipole operator. Their results with this ground state and the exact final state described above (note that the wave functions are not eigenstates of the same Hamiltonian due to the *ad hoc* nature of the ground state) agree with the total-cross-section data of Fetisov, Gorbunov, and Varfolomeev,[2] but not the data for the 90° differential cross section of Stewart, Morrison, and O'Connell[3] or Berman, Koester, and Smith[4] which lie ~20% below the calculated curve at the peak. Barbour and Phillips then conclude that since their ground state gives a reasonable fit to the ^{3}He charge form factor out to four-momentum transferred squared ~3 fm^{-2}, the 90° two-body photodisintegration data are incompatible with the charge form factor.

Since the work in Ref. 1, there have been a number of new experiments. The first was a radiative proton-deuteron capture experiment[5] which indicated possible structure in the equivalent (converted by detailed balance) 90° photodisintegration cross section at $E_\gamma \approx 20$ MeV. A number of experiments followed in an attempt to verify the apparent structure in the 90° cross section. Two of these were radiative capture experiments,[6,7] three were electrodisintegration experiments[8-10] where only the deuteron is detected with the re-

sults converted to equivalent photodisintegration cross sections by application of the virtual-photon approximation, and one was a photodisintegration experiment.[11] In only one of these experiments do the data indicate possible structure,[6] but at a lower energy—$E_\gamma \approx 14$ MeV—than the original capture experiment of Ref. 5. In fact, the consensus supports no evidence for structure in the low-energy 90° photodisintegration energy spectrum. Moreover, the above experiments serve another purpose: They provide data concerning the apparent normalization discrepancy pointed out by Barbour and Phillips between the previous total cross section measurements and 90° data. Nevertheless, the new data do not resolve the conflict. The new data fall into two groups: (1) The electrodisintegration data[9,10] and the Halbert *et al.*[5] capture data support the larger peak value of the Fetisov *et al.*[2] total cross section measurements; (2) the photodisintegration experiment of Ticcioni *et al.*[11] and the capture data of Chang, Diener, and Ventura[6] agree with the early 90° results.[3,4] A more recent capture experiment by Matthews *et al.*[12] designed to check the normalization at one photon energy point, $E_\gamma = 16.1$ MeV, falls into the second group. The point these data seem to raise concerns the validity of the virtual-photon approximation in converting the electrodisintegration data to an equivalent photodisintegration cross section—a question which falls mainly in the theoretical realm.

Recent theoretical effort on the two-body photodisintegration process has centered on extending the work of Barbour and Phillips. Barbour and Hendry[13] add the electric quadrupole amplitude and find its effect on the total cross section to be negligible for $E_\gamma \lesssim 40$ MeV. Hendry and Phillips[14] include the tensor force in obtaining the exact final state and construct, in a manner similar to Barbour and Phillips,[15] a ^{3}He ground-state wave function including a D-state component. As the percentage deuteron D state takes on the values 0, 4, and 7% with the percentage D state in ^{3}He being 0, 4.03, and 7.71%, respectively, the peak of the 90° two-body photodisintegration cross section decreases from ~120 μb/sr to ~100 μb/sr compared to the 90° measurements which favor a peak value between ~85 to 90 μb/sr. The Hendry-Phillips calculations also include a proton-deutron Coulomb correction which, if removed, would raise their values by 7%. They also argue that a complete separable-potential calculation, i.e., including tensor forces and short-range effects, cannot be expected to give a peak value much less than ~105 μb/sr. To support this contention, they point out that the $^3\mathrm{He} \to p + d$ vertex may be overestimated by separable-potential models. Using a related quantity as a gauge—the residue at the triton pole in the center-of-mass n-d scattering amplitude, they calculate with their *ad hoc* ground-state wave functions a value for the residue $R = -4.6\ \mathrm{fm}^{-1}$, which they compare to $R = -3.2 \pm 0.4\ \mathrm{fm}^{-1}$ extracted from experiment by Locher.[16]

The objectives of our paper are threefold: (1) to present an alternative method (from that of Barbour and Phillips) for performing the exact two-body ^{3}He photodisintegration calculation; (2) to consider the effect of charge-dependent two-nucleon interactions on the photodisintegration predictions including differences to be expected between ^{3}He and ^{3}H; and (3) to emphasize that the photodisintegration calculations and the residue calculations are sensitive to the form of the spectator functions in the separable-model ground-state wave function. We present our three-body formalism in Sec. II and apply it to ^{3}He(^{3}H) photodisintegration in Sec. III. Sections IV, V, and VI contain our results, discussion, and conclusions, respectively. Two appendices are included to describe our numerical methods and to give the relationship between the residue at the triton pole in the n-d scattering amplitude and the asymptotic normalization constant of the n-d tail in the trition ground-state wave function.

II. FORMALISM

In this section, we develop the formalism for the disintegration of a three-body nucleus by an interaction which can be treated perturbatively, e.g., disintegration by the electromagnetic or weak interaction. Explicit in our treatment will be the assumption that the two-body nuclear interaction can produce a two-body bound state.

Consider the total Hamiltonian

$$H_{\mathrm{total}} = H + H' \ , \tag{1}$$

where H' is the interaction to be treated perturbatively and H is the nuclear Hamiltonian composed of kinetic energy and pair interaction operators, i.e.,

$$H = H_0 + V \tag{2}$$

with

$$V = \sum_{\alpha=1}^{3} V_\alpha = V_1 + V_2 + V_3 \equiv V_{23} + V_{31} + V_{12} \ . \tag{3}$$

Specifically, the nuclear Hamiltonian will be assumed to have eigenstates corresponding to a three-body bound state, a scattering state of a particle plus bound pair, and a scattering state of three unbound particles. For these states, respec-

tively, we have

$$H|\Psi_B\rangle = -E_B|\Psi_B\rangle, \quad E_B > 0; \tag{4}$$

$$H|\Psi_{\alpha n\vec{p}}\rangle = E^{(2)}_{\alpha n}|\Psi_{\alpha n\vec{p}}\rangle, \quad E^{(2)}_{\alpha n} = \frac{p^2}{2m_\alpha} - \epsilon_{\alpha n}, \quad \epsilon_{\alpha n} > 0; \tag{5}$$

$$H|\Psi_{\alpha n\vec{p}\vec{k}}\rangle = E^{(3)}_{\alpha n}|\Psi_{\alpha n\vec{p}\vec{k}}\rangle, \quad E^{(3)}_{\alpha n} = \frac{p^2}{2m_\alpha} + \frac{k^2}{2\mu_\alpha}; \tag{6}$$

where, for example, the subscripts in Eq. (6) mean particle α moves relative to the center of mass of pair $\beta\gamma$ ($\alpha \neq \beta \neq \gamma \neq \alpha$ and each can take on the values 1 to 3) with relative momentum $\vec{p}$, while $\beta\gamma$ move relative to each other with momentum $\vec{k}$, and n describes the remaining quantum numbers of the state such as spin and isospin. The reduced masses are given by $m_\alpha = M_\alpha(M_\beta + M_\gamma)/\sum_{\alpha=1}^{3} M_\alpha$ and $\mu_\alpha = M_\beta M_\gamma/(M_\beta + M_\gamma)$, where M_α denotes the mass of particle α.

In this paper dealing with two-body photodisintegration of ^{3}He and ^{3}H, we are concerned only with two-body disintegration amplitudes

$$A_2(\alpha, n, \vec{p}) = \langle \Psi^{(-)}_{\alpha n\vec{p}}|H'|\Psi_B\rangle, \tag{7}$$

where the superscript (−) denotes the outgoing state which asymptotically corresponds to an incoming wave. The two-body scattering state is a solution of the equivalent equations ($\eta > 0$; $E = p^2/2m_\alpha - \epsilon_{\alpha n}$)

$$|\Psi^{(-)}_{\alpha n\vec{p}}\rangle = |\Phi_{\alpha n\vec{p}}\rangle - G_\alpha(E - i\eta)\sum_{\beta\neq\alpha} V_\beta|\Psi^{(-)}_{\alpha n\vec{p}}\rangle \tag{8}$$

and

$$|\Psi^{(-)}_{\alpha n\vec{p}}\rangle = |\Phi_{\alpha n\vec{p}}\rangle - G(E - i\eta)\sum_{\beta\neq\alpha} V_\beta|\Phi_{\alpha n\vec{p}}\rangle, \tag{9}$$

with the resolvent operators defined as

$$G_\alpha(z) = (H_0 + V_\alpha - z)^{-1}, \tag{10}$$

$$G(z) = (H - z)^{-1}, \tag{11}$$

and $|\Phi_{\alpha n\vec{p}}\rangle$ denoting the asymptotic scattering state composed of particle α moving freely relative to the $\beta\gamma$ bound pair. If Eq. (9) is written in terms of the distortion operator

$$\bar{\Omega}^{(-)}_\alpha \equiv \bar{\Omega}_\alpha(E - i\eta) = 1 - G(E - i\eta)\sum_{\beta\neq\alpha} V_\beta \tag{12}$$

and substituted into Eq. (7), we obtain

$$A_2(\alpha, n, \vec{p}) = \langle \Phi_{\alpha n\vec{p}}|\Omega^{(+)}_\alpha H'|\Psi_B\rangle, \tag{13}$$

where $\Omega^{(+)}_\alpha = (\bar{\Omega}^{(-)}_\alpha)^\dagger$. The crux of this development is that a Faddeev-type equation can be written for $\Omega^{(+)}_\alpha$:

$$\Omega^{(+)}_\alpha = (\bar{\Omega}^{(-)}_\alpha)^\dagger = 1 - \sum_{\beta\neq\alpha} V_\beta G(E + i\eta)$$

$$= G_\alpha^{-1}(E + i\eta)G(E + i\eta) \tag{14}$$

$$= 1 - \sum_{\beta\neq\alpha} V_\beta G_\beta G_\beta^{-1} G \tag{15}$$

$$= 1 - \sum_{\beta\neq\alpha} V_\beta G_\beta \Omega^{(+)}_\beta. \tag{16}$$

Equation (16) can then be written in terms of the two-body T operator

$$\Omega^{(+)}_\alpha = 1 - \sum_{\beta=1}^{3} \tilde{\delta}_{\alpha\beta} T_\beta G_0 \Omega^{(+)}_\beta, \tag{17}$$

since

$$T_\beta(z)G_0(z) = V_\beta G_\beta(z), \tag{18}$$

where $\tilde{\delta}_{\alpha\beta} = 1 - \delta_{\alpha\beta}$ and $G_0(z) = (H_0 - z)^{-1}$. When Eq. (17) is substituted into Eq. (13), a set of coupled (integral) equations for the two-body off-shell disintegration amplitudes is obtained. This was the route followed by Barbour and Phillips in their treatment of ^{3}He photodisintegration.[1] However, we shall use Eq. (17) to express Eq. (13) in terms of the half-off-shell particle-plus-correlated-pair scattering amplitude. One way in which this can be achieved is by iterating Eq. (17) to obtain

$$\Omega^{(+)}_\alpha = 1 - \sum_{\beta=1}^{3} \tilde{\delta}_{\alpha\beta} T_\beta G_0 + \sum_{\beta=1}^{3}\sum_{\gamma=1}^{3} \tilde{\delta}_{\alpha\beta} T_\beta G_0 \tilde{\delta}_{\beta\gamma} T_\gamma G_0 - + \cdots, \tag{19}$$

then grouping terms as

$$\Omega^{(+)}_\alpha = 1 - \sum_{\gamma=1}^{3} (\tilde{\delta}_{\alpha\gamma} - \sum_{\beta=1}^{3} \delta_{\alpha\beta} T_\beta G_0 \delta_{\beta\gamma} + - \cdots) T_\gamma G_0 \tag{20}$$

and recognizing the parenthetical expression in Eq. (20) as $G_0^{-1}X_{\alpha\gamma}$, where $X_{\alpha\gamma}$ is the transition operator that connects particle-plus-correlated-pair states.[17] Therefore,

$$\Omega^{(+)}_\alpha = 1 - \sum_{\gamma=1}^{3} G_0^{-1} X_{\alpha\gamma} T_\gamma G_0, \tag{21}$$

where

$$X_{\alpha\beta}(z) = G_0(z)\tilde{\delta}_{\alpha\beta} - \sum_\gamma X_{\alpha\gamma}(z) T_\gamma(z) \tilde{\delta}_{\gamma\beta} G_0(z) \tag{22}$$

or

$$X_{\alpha\beta}(z) = G_0(z)\tilde{\delta}_{\alpha\beta} - G_0(z)\sum_\gamma \tilde{\delta}_{\alpha\gamma} T_\gamma(z) X_{\gamma\beta}(z). \tag{23}$$

The three-particle dynamics of the continuum state now reside in the transition operators $X_{\alpha\gamma}$ and the two-body disintegration amplitude is written

$$A_2(\alpha, n, \vec{p}) = \langle \Phi_{\alpha n \vec{p}} | H' | \Psi_B \rangle - \sum_{\gamma=1}^{3} \langle \Phi_{\alpha n \vec{p}} | G_0^{-1}(z) X_{\alpha\gamma}(z) T_\gamma(z) G_0(z) H' | \Psi_B \rangle \ , \tag{24}$$

with $z = p^2/2m_\alpha - \epsilon_{\alpha n} + i\eta$.

The utility of expression the two-body disintegration amplitude in terms of the transition operator that connects particle-plus-correlated-pair states will become clear in the following section, but already it is evident that the three-particle dynamics have been separated from the disintegration process due to H'. In effect, the continuum three-body problem need only be considered once for a given excitation energy to handle all weak disintegration processes. As will be shown in the second paper of this series, this is, of course, also the case for three-body disintegration processes. Moreover, we emphasize that this approach is completely equivalent to that of Barbour and Phillips, and corresponds to using the exact three-body eigenstates in computing the amplitude of Eq. (7).

III. APPLICATION OF THE FORMALISM TO THE TWO-BODY PHOTODISINTEGRATION OF ^{3}He AND ^{3}H

A. Spin-dependent charge-independent interactions

The application of Eq. (24) to the two-body photodisintegration of ^{3}He and ^{3}H requires knowledge of $T_\alpha(z)$ and H'. The two-nucleon transition operator in the three-particle Hilbert space $T_\alpha(z)$ will first be taken to be representable as an attractive s-wave spin-dependent separable form. We shall write

$$T_\alpha(z) = -\sum_{n=s}^{t} |g_{\alpha n}\rangle \tau_{\alpha n}(z) \langle g_{\alpha n}| (|SI\rangle\langle SI|)_{\alpha n} \ , \tag{25}$$

where

$$\tau_{\alpha n}(z) = \frac{\lambda_n}{2\mu_\alpha} \left(1 + \frac{\lambda_n}{2\mu_\alpha} \int d^3p \, \frac{g_n^2(p)}{z - p^2/2\mu_\alpha} \right)^{-1} \tag{26}$$

and

$$g_{\alpha n}(p) = \langle \vec{p} | g_{\alpha n} \rangle \ . \tag{27}$$

The lower-case letters s and t stand for singlet and triplet spin, respectively; the upper-case letter $S(I)$ is the total spin (isospin) obtained by first coupling the spins (isospins) of particles β and γ, and then coupling their resultant spin (isospin) to the spin (isospin) of particle α to form the total $S(I)$; and λ_n represents the strength of the interaction. The momentum dependent form factors $g_{\alpha n}(p)$ determine the ranges of the interactions. This form of the two-nucleon interaction corresponds to a separable, nonlocal potential which, if it can support a bound state of binding energy ϵ_n, yields for the bound-state wave function

$$\langle \chi_n | = N_2 \langle g_n | G_0^{(2)}(-\epsilon_n); \quad \epsilon_n > 0 \ , \tag{28}$$

where N_2 is the normalization constant to assure $\langle \chi_n | \chi_n \rangle = 1$ and $G_0^{(2)}(z)$ is the free-particle resolvent for two particles [in contrast to $G_0(z)$ which is the free-particle resolvent for *three* particles]. Then the state of interest to us becomes

$$\langle \Phi_{\alpha n \vec{p}} | = N_2 \langle g_{\alpha n} \vec{p} | G_0 \left(\frac{p^2}{2m_\alpha} - \epsilon_{\alpha n} \right) \tag{29}$$

with $\langle g_{\alpha n} \vec{p}| = \langle g_{\alpha n} | \langle \vec{p}|$. Equations (25) and (29) along with $H' = H_{\rm em}$ (to be specified in more detail below) permit us to write Eq. (24) as

$$A_2(\alpha, n, \vec{p}) = N_2 \left[\langle g_{\alpha n} \vec{p} | G_0(z) H_{\rm em} | \Psi_B \rangle + \sum_{\beta=1}^{3} \sum_{n'=s}^{t} \int d^3p' \langle g_{\alpha n} \vec{p} | X_{\alpha\beta}(z) | g_{\beta n'} \vec{p}' \rangle \tau_{\beta n'} \left(z - \frac{p'^2}{2m_\beta} \right) \langle g_{\beta n'} \vec{p}' | G_0(z) H_{\rm em} | \Psi_B \rangle \right], \tag{30}$$

where the spin-isospin projection operator is suppressed in the second term, $\int d^3p' |\vec{p}' \times \vec{p}'| = 1$ has been used, and $z = p^2/2m_\alpha - \epsilon_{\alpha n} + i\eta$.

The next step in applying the formalism to the two-body photodisintegration of ^{3}He and ^{3}H is to utilize the fact that the nucleons will be treated as three identical particles of mass M. We obtain symmetrized expressions from Eq. (30) as follows:

$$M_2^n(z, \vec{p}) \equiv \sqrt{\tfrac{1}{3}} \sum_{\alpha=1}^{3} A_2(\alpha, n, \vec{p}) \tag{31}$$

$$= B_n(z, \vec{p}) + \sum_{n'=s}^{t} \int d^3p' \langle \vec{p} | X_{nn'}(z) | \vec{p}' \rangle \times \tau_{n'} \left(z - \frac{3p'^2}{4M} \right) B_{n'}(z, \vec{p}') \ , \tag{32}$$

where $z = 3p^2/4M - \epsilon_d + i\eta$ and the deuteron binding energy $\epsilon_d \equiv \gamma^2/M = 2.225$ MeV. The amplitudes appearing in Eq. (32) written in off-shell form (i.e., z in general not equal to $3p^2/4M - \epsilon_d + i\eta$ and $|\vec{p}|$ not necessarily the same as $|\vec{p}'|$) are

$$B_n(z, \vec{p}) = N_2\sqrt{\tfrac{1}{3}} \sum_{\alpha=1}^{3} \langle g_{\alpha n}\vec{p} | G_0(z) H_{\rm em} | \Psi_B \rangle \qquad (33)$$

and

$$\langle \vec{p} | X_{nn'}(z) | \vec{p}' \rangle = \frac{1}{3} \sum_{\alpha=1}^{3} \sum_{\beta=1}^{3} \langle g_{\alpha n}\vec{p} | X_{\alpha\beta}(z) | g_{\beta n'}\vec{p}' \rangle \ . \qquad (34)$$

The off-shell three-particle transition amplitude $\langle \vec{p} | X_{nn'}(z) | \vec{p}' \rangle$ satisfies the integral equation

$$\langle \vec{p} | X_{nn'}(z) | \vec{p}' \rangle = \langle \vec{p} | Z_{nn'}(z) | \vec{p}' \rangle + \sum_{m=s}^{t} \int d^3p'' \langle \vec{p} | X_{nm}(z) | \vec{p}'' \rangle \tau_m \left(z - \frac{3p''^2}{4M} \right) \langle \vec{p}'' | Z_{mn'}(z) | \vec{p}' \rangle \ , \qquad (35)$$

where

$$\langle \vec{p} | Z_{nn'}(z) | \vec{p}' \rangle = \frac{1}{3} \sum_{\alpha=1}^{3} \sum_{\beta=1}^{3} \tilde{\delta}_{\alpha\beta} \langle g_{\alpha n}\vec{p} | G_0(z) | g_{\beta n'}\vec{p}' \rangle \ . \qquad (36)$$

Equation (35) is derived from Eq. (22) using the definition Eq. (34).

The method we use to obtain the two-body disintegration amplitude is now clear on the basis of Eqs. (32) and (35). This can be made even more vivid by representing these equations graphically as in Fig. 1. Figure 1(a) illustrates our method and Fig. 1(b) the method of Barbour and Phillips.[1] The point to note is that by our method all two-body disintegration processes are obtained by solving the *same* equation [Eq. (35)] for the three-

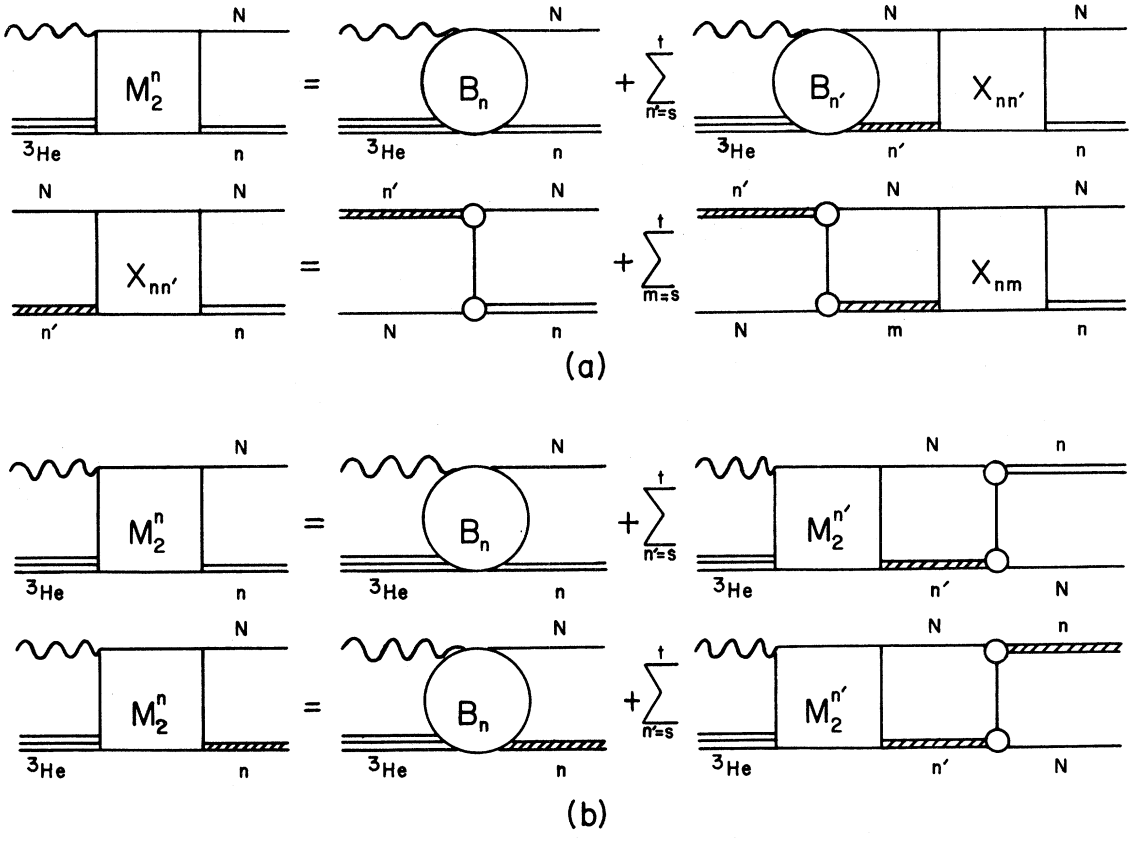

FIG. 1. Comparison of the equations used to obtain the two-body disintegration amplitude in this work, (a), with those of Barbour and Phillips, Ref. 1, (b). The wavy line represents the disintegration mechanism (e.g., in the case of photodisintegration a photon) and the cross-hatched double lines are to indicate that a particular correlated pair plus nucleon (N) are off shell. In the case of ^{3}He photodisintegration into proton plus deuteron, N = proton and n = triplet or the plain double lines represent the deuteron.

particle continuum dynamics, while the type of process is governed by the Born amplitude $B_n(z,\vec{p})$. In contrast, Barbour and Phillips solve an integral equation for the off-shell amplitude $M_2^n(z,\vec{p})$ and use this amplitude in the same equation with the external variables on-shell to obtain by an integration the on-shell amplitude $M_2^n(z=3p^2/4M-\epsilon_d,\vec{p})$.

The last major step in our application of the formalism involves the details of $B_n(z,\vec{p})$, or equivalently, the specification of $H'=H_{\rm em}$ [see Eq. (33)]. It is a well-established fact that the two-body photodisintegration of ^{3}He is mainly an electric-dipole transition,[18] so we take

$$H'=H_{\rm em}=\frac{1}{2}e\sum_{i=1}^{3}(\hat{\epsilon}\cdot\vec{r}_i)\tau_3^{(i)}\equiv\mathfrak{D}\ , \tag{37}$$

where the $\vec{r}_i$ are the nucleon center-of-mass coordinates, $\hat{\epsilon}$ is the photon-polarization unit vector, e is the electric charge, and $\tau_3^{(i)}$ is the third (z-component) isospin Pauli matrix for particle i. In this work, we include only the dominant component of the ^{3}He ground-state wave function, namely, the $^2S_{1/2}$ spatially symmetric one. The ground state of ^{3}He can then be written

$$|\Psi_B\rangle=\Psi_0^s\sqrt{\tfrac{1}{2}}(\chi'\eta''-\chi''\eta')\ , \tag{38}$$

where Ψ_0^s is the symmetric spatial part, $\chi'(1,\widehat{23})$ $[\eta'(1,\widehat{23})]$ is the spin-$\frac{1}{2}$ [isospin-$\frac{1}{2}$] function obtained by first coupling the spins [isospins] of nucleons 2 and 3 to spin [isospin] zero, and $\chi''(1,\overline{23})$ $[\eta''(1,\overline{23})]$ is the spin-$\frac{1}{2}$ [isospin-$\frac{1}{2}$] function obtained by first coupling the spins [isospins] of nucleons 2 and 3 to spin [isospin] one. Combining Eqs. (37) and (38), we get

$$\mathfrak{D}|\Psi_B\rangle=\left(\frac{-e}{2\sqrt{3}}\right)\hat{\epsilon}\cdot\left[\frac{2}{\sqrt{3}}\vec{\rho}\xi'-\vec{r}\xi''-\left(\frac{2}{\sqrt{3}}\vec{\rho}\chi'-\vec{r}\chi''\right)\eta^s\right]\Psi_0^s\ . \tag{39}$$

In Eq. (39), $\vec{r}$ and $\vec{\rho}$ are the standard Jacobi variables for three identical particles, e.g.,

$$\vec{r}=\vec{r}_2-\vec{r}_3\ , \tag{40a}$$

$$\vec{\rho}=\vec{r}_1-\tfrac{1}{2}(\vec{r}_2+\vec{r}_3)=\tfrac{3}{2}\vec{r}_1\ , \tag{40b}$$

η^s is the isospin-$\frac{3}{2}$ function for three nucleons, and

$$\xi'=\frac{1}{\sqrt{2}}(\chi'\eta''+\chi''\eta')\ , \tag{41a}$$

$$\xi''=\frac{1}{\sqrt{2}}(\chi'\eta'-\chi''\eta'')\ . \tag{41b}$$

With Eqs. (39)–(41), it is then easy to obtain $B_t(z,\vec{p})$ for the two-body photodisintegration of ^{3}He. The final-state spin-isospin projection in Eq. (33) is $\chi''\eta'$ and since the deuteron wave function is s wave, we get

$$B_t(z,\vec{p})=\frac{-eMN_2}{\sqrt{6}}\int d^3k\,\frac{g_t(k)[\hat{\epsilon}\cdot\vec{\rho}_{0p}\Psi_0^s(\vec{k},\vec{p})]}{3p^2/4+k^2-Mz}\ , \tag{42}$$

where $\vec{\rho}_{0p}=-i\hbar\vec{\nabla}_p$. The electric-dipole operator connects the $^2S_{1/2}$ ground state with a ^2P continuum state.

Using the fact that the p-d (or n-d) final state in the ^{3}He (^{3}H) electric-dipole photodisintegration is p wave, we specialize Eqs. (32), (35), and (36) to a practical form by defining

$$B_n(z,\vec{p})=\hat{\epsilon}\cdot\hat{p}\,\mathfrak{B}_n(z,p) \tag{43}$$

and using the partial-wave decompositions

$$\langle\vec{p}|X_{nn'}(z)|\vec{p}'\rangle=\sum_{J=0}^{\infty}(2J+1)X_{nn'}^J(p,p';z)P_J(\hat{p}\cdot\hat{p}')\ , \tag{44}$$

$$\langle\vec{p}|Z_{nn'}(z)|\vec{p}'\rangle=\sum_{J=0}^{\infty}(2J+1)Z_{nn'}^J(p,p';z)P_J(\hat{p}\cdot\hat{p}')\ . \tag{45}$$

$P_J(\cos\theta)$ is the Legendre function for angular momentum J. After some algebra, we get for the two-body ^{3}He photodisintegration amplitude

$$M_2^t(z,\vec{p})=\hat{\epsilon}\cdot\hat{p}\left[\mathfrak{B}_t(z,p)+4\pi\sum_{n=s}^{t}\int_0^\infty p'^2dp'X_{tn}^1(p,p';z)\tau_n\left(z-\frac{3p'^2}{4M}\right)\mathfrak{B}_n(z,p')\right] \tag{46}$$

$$\equiv\hat{\epsilon}\cdot\hat{p}\,\mathfrak{M}_2^t(z,p)\ . \tag{47}$$

We note that $\mathfrak{B}_s(z,p)$ is present in Eq. (46) and that it can be obtained in the same manner as $\mathfrak{B}_t(z,p)$, i.e., project with $\chi'\eta''$ in Eq. (33) to obtain the same result as Eq. (42) except $g_t(k)$ is replaced by $g_s(k)$. The amplitudes $X_{tt}^1(p,p';z)$ and $X_{ts}^1(p,p';z)$ are obtained from the coupled integral equations

$$X_{nn'}^1(p,p';z)=Z_{nn'}^1(p,p';z)+4\pi\sum_{m=s}^{t}\int_0^\infty p''^2dp''Z_{n'm}^1(p',p'';z)\tau_m\left(z-\frac{3p''^2}{4M}\right)X_{nm}^1(p,p'';z)\ , \tag{48}$$

where

$$Z^J_{nn'}(p,p';z)=C_{nn'}\int_{-1}^{1}dx\,\frac{P_J(x)g_n(q^2)g_{n'}(q'^2)}{p^2+p'^2+pp'x-Mz}\ , \tag{49a}$$

$$q^2=\tfrac{1}{4}p^2+p'^2+pp'x\ , \tag{49b}$$

$$q'^2=p^2+\tfrac{1}{4}p'^2+pp'x\ , \tag{49c}$$

and use was made of the relation

$$Z^J_{nn'}(p,p';z)=Z^J_{n'n}(p',p;z)\ . \tag{50}$$

The coefficient matrix is

$$[C_{nn'}]=\begin{pmatrix}C_{tt} & C_{ts}\\ C_{st} & C_{ss}\end{pmatrix}=\begin{pmatrix}\frac{1}{4} & -\frac{3}{4}\\ -\frac{3}{4} & \frac{1}{4}\end{pmatrix}. \tag{51}$$

Once the amplitude $M_2^t(z,\vec{p})$ has been obtained from Eqs. (46)–(51) (see Appendix A concerning our numerical methods), it can be related to the two-body differential cross section in the standard way:

$$d\sigma=\frac{2\pi^2}{\hbar c}E_\gamma\left|\mathfrak{M}^t_2\left(\frac{3p^2}{4M}-\frac{\gamma^2}{M},p\right)\right|^2\sin^2\theta\rho_f\ , \tag{52}$$

where E_γ is the photon energy, θ is the center-of-mass angle of the outgoing nucleon with respect to the incident photon direction, and ρ_f is the density of final states

B. Spin-dependent charge-dependent interactions

The generalization of part A of this section to spin-dependent charge-dependent interactions occurs through Eq. (25). Instead of the summation in Eq. (25) including singlet and triplet terms with no distinction between the n-n, n-p, and p-p singlets, it now distinguishes the various singlet pieces. The completely symmetric part of the ^{3}He wave function in momentum space generalizes to

$$\Psi^s_0(\vec{k},\vec{p})=\Psi^{(1)}+\Psi^{(2)}+\Psi^{(3)}\ , \tag{53a}$$

$$\Psi^{(1)}=N_3\frac{g^t_{np}(k)u^t_{np}(p)+\frac{1}{3}g^s_{np}(k)u^s_{np}(p)+\frac{2}{3}g_{pp}(k)u_{pp}(p)}{k^2+\frac{3}{4}p^2+ME_B} \tag{53b}$$

as given by Gibson and Stephenson[19] (for ^{3}H, everywhere exchange $p\rightleftarrows n$).[20] When the n-p singlet and p-p singlet interactions are taken to be identical, Eq. (53b) reduces to the standard charge-independent form of Sitenko and Kharchenko.[21] The generalizations in Eqs. (46) and (48) follow directly from changing the $\sum_{n=s}^{t}$. The coefficient matrix for the case of two protons and a neutron becomes

$$[C_{nn'}]=\begin{pmatrix}C_{tt} & C_{s_{np}t} & C_{s_{pp}t}\\ C_{ts_{np}} & C_{s_{np}s_{np}} & C_{s_{pp}s_{np}}\\ C_{ts_{pp}} & C_{s_{np}s_{pp}} & C_{s_{pp}s_{pp}}\end{pmatrix}=\begin{pmatrix}\frac{1}{4} & -\frac{1}{4} & -\frac{1}{2}\\ -\frac{3}{4} & -\frac{1}{4} & \frac{1}{2}\\ -\frac{3}{4} & \frac{1}{4} & 0\end{pmatrix}. \tag{54}$$

IV. RESULTS

In our calculations of the two-body photodisintegration 90° differential cross sections for ^{3}He and ^{3}H, several sets of two-nucleon parameters have been used to generate the three-body ground-state and continuum wave functions. All sets are obtained by requiring the separable interactions to reproduce various values for the two-nucleon effective-range parameters. Table I lists these parameters along with the corresponding two-nucleon scattering lengths and effective ranges.[22] The binding energies for the three-body ground states predicted on the basis of several different combinations of these interactions are given in Table II, along with the charge radii computed from the spatially symmetric part of the corresponding wave function. For completeness, we have included the normalization constant N_3, the values of the parameters obtained in fitting the spectator functions $u(p)$ to the analytic form const./$(1+\bar{\alpha}p^2+\bar{\beta}p^4+\bar{\gamma}p^6)$, and C^2, the square of the asymptotic normalization constant for the nucleon-deuteron tail in the ground-state wave function. (See Appendix B for the definition of C and its computation.) We give the same information for two wave functions where the triplet two-nucleon strength parameter has been weakened slightly to reproduce the experimental ^{3}He and ^{3}H binding energies. This adjustment partly simulates the effect of the tensor component of the triplet two-nucleon interaction which we have not included. Also shown in Table II are the wave functions of Barbour and Phillips which they label I.[23]

The first computation carried out was to assure that our results were consistent with those of Barbour and Phillips. To this end, we used their ^{3}He ground-state wave function given in Table II plus two-nucleon parameters in the final state which were identical to theirs for the triplet, set III in Table I, and only slightly different for the singlet. The parameters they used for the two-nucleon singlet correspond to $a=-20.34$ fm and $r_0=2.7$ fm, whereas ours were n-p singlet set II in Table I. This slight deviation from their singlet parameters makes essentially no difference in the final result, since the calculation is not sensitive to small

TABLE I. Parameters for separable interactions.

Interaction		Strength λ (fm^{-3})	Inverse range [a] β (fm^{-1})	Scattering length a (fm)	Effective range r_0 (fm)
s wave n-p triplet [b]	I	0.3815	1.406	5.423	1.761
	II	0.220	1.15	5.68	2.09
	III	0.391	1.418	5.397	1.747
s wave n-p singlet	I	0.1445	1.153	−23.715	2.74
	II	0.148	1.15	−21.25	2.74
s wave p-p singlet		0.1534	1.223	−7.823	2.794
s wave n-n singlet		0.1323	1.130	−17.0	2.84

[a] The standard s-wave form for the functions $g_n(p)$, Eq. (27), is used, i.e., $g_n(p) = (p^2 + \beta_n^2)^{-1}$.
[b] The deuteron binding energy is 2.225 MeV.

changes in the final-state parameters. There are small differences between our result and theirs which are probably attributable to numerics. We shall not show the comparison since it has already appeared in the paper by Chang, Dodge, and Murphy on the ^{3}He$(\gamma, d)^1$H reaction between 10 and 21 MeV.[10,24]

In our first set of new computations, three comparisons are made: (1) the effect of changing the kinematics to reflect the difference in the ^{3}He and ^{3}H photoreaction thresholds, everything else remaining the same; (2) the differences which occur when the ground-state wave function is obtained from an average of the singlet and triplet two-nucleon interactions (mixed-symmetry component identically zero) as opposed to distinguishing the singlet and triplet strengths; (3) the result of arbitrarily changing the binding-energy parameter

TABLE II. ^{3}He and ^{3}H ground-state wave functions.

Wave function [a]	Interaction set	Binding energy (MeV)	Charge radius (fm) [b]	C^2	N_3 (fm^{-1}) [c]	Spectator function parameters Const.	$\bar{\alpha}$	$\bar{\beta}$	$\bar{\gamma}$
Symmetric Tabakin	Average of n-p triplet and singlet sets II	9.33	1.75	2.67	0.3235	1.0	3.670	1.469	0.1620
Tabakin	n-p triplet and singlet sets II	10.1	1.74	3.32	0.2268	1.0 0.4907	4.255 2.989	1.930 1.170	0.1538 0.0984
Charge dependent ^{3}H	n-p triplet I n-p singlet I n-n singlet	10.34	1.65	2.60	0.3163	1.0 0.3207 0.2965	4.142 2.730 2.690	1.651 0.7838 0.7582	0.1037 0.0655 0.0650
Charge dependent ^{3}H (adjusted)	n-p triplet $\lambda = 0.3608$ fm^{-3} n-p singlet I n-n singlet	8.49	1.74	2.58	0.3063	1.0 0.3520 0.3249	4.617 3.181 3.129	1.801 0.8879 0.8545	0.1208 0.0815 0.0809
Charge dependent ^{3}He (adjusted)	n-p triplet $\lambda = 0.3589$ fm^{-1} n-p singlet I p-p singlet	7.71	1.77	2.39	0.3159	1.0 0.3485 0.3272	5.035 3.403 3.207	1.830 0.8662 0.8090	0.1272 0.0868 0.0788
Barbour-Phillips I-^{3}H	•••	8.49	1.63	3.84	0.3611	1.0 0.3097	5.464 3.949	2.545 1.067	0.3103 0.0748
Barbour-Phillips I-^{3}He	•••	7.71	1.87	3.26	0.3721	1.0 0.3095	6.151 4.310	2.888 1.170	0.3532 0.08214

[a] The charge radius, C^2, and N_3 are computed from the spatially symmetric component of the wave function, except for the charge radii of the Barbour-Phillips wave functions which include the mixed symmetry component.
[b] We assume the proton charge radius is 0.8 fm and the neutron charge radius is zero. Barbour and Phillips take the proton charge radius to be 0.848 fm and the neutron mean-square charge radius to be −0.1258 fm^2. The experimental charge radii of ^{3}He and ^{3}H obtained by Collard *et al.*, are 1.87 ± 0.05 fm and 1.70 ± 0.05 fm, respectively (Ref. 25).
[c] See Eqs. (53).

from the theoretical value to the experimental value. These results are presented in Fig. 2 where (1) is seen by comparing curves I and II, (2) by comparing I and III, and (3) by comparing III and IV. The ground-state wave functions used in calculating these curves are given in the figure caption while the charge-independent final-state two-nucleon parameters remained the same throughout and were n-p triplet and singlet sets II.

Next, we investigated the differences to be expected between ^{3}He and ^{3}H; initially using the Barbour-Phillips ^{3}He and ^{3}H wave functions, and after that, with our charge-dependent (adjusted) wave functions. Figure 3 displays the results obtained with the Barbour-Phillips wave functions where curves I and III are for ^{3}He and curves II and IV for ^{3}H. The final-state parameters are n-p triplet and singlet sets II for curves I and II, and the charge-dependent combinations made from n-p triplet and singlet sets I combined with either the p-p or n-n singlet parameters depending on whether the initial state was ^{3}He or ^{3}H, respectively. Thus, besides being able to compare differences between ^{3}He and ^{3}H by comparing either curves I and II or III and IV, respectively, we can estimate the effect of using charge-dependent two-nucleon interactions in the final state by comparing either curves I and III or II and IV. In Fig. 4, we display our curves obtained with the charge-dependent final-state parameters and the ^{3}He and ^{3}H charge-dependent (adjusted) wave functions. This represents our best estimate of the difference to be expected between the ^{3}He and ^{3}H two-body photodisintegration cross sections.

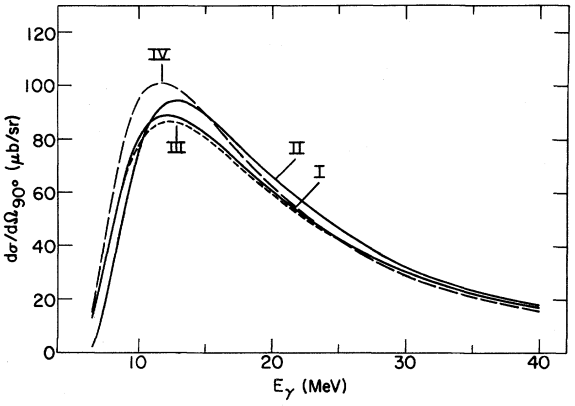

FIG. 2. Two-body 90° photodisintegration cross section for (I) ^{3}He(γ, d), symmetric Tabakin ground state, (II) ^{3}H(γ, d), symmetric Tabakin ground state, (III) ^{3}He(γ, d), Tabakin ground state, and (IV) ^{3}He(γ, d), Tabakin ground state with binding-energy parameter arbitrarily set to the experimental value. The two-nucleon final-state parameters are the same throughout; i.e., n-p triplet and singlet sets II.

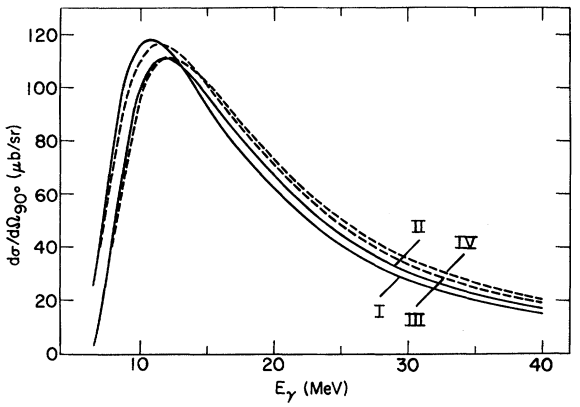

FIG. 3. Two-body 90° photodisintegration cross sections with the Barbour-Phillips ground states. Curves I and III are ^{3}He, while II and IV are ^{3}H. The two-nucleon final-state parameters are n-p triplet and singlet sets II for curves I and II, and the charge-dependent sets made from n-p triplet and singlet sets I combined with either the p-p or n-n singlet parameters for curves III and IV, respectively.

The difference between our fully charge-dependent calculation and the Barbour-Phillips calculation for ^{3}He is displayed in Fig. 5 along with the available ^{3}He$(\gamma, d)p$ data. The curve with the highest peak is the same as curve I in Fig. 3 which is obtained from the Barbour-Phillips ^{3}He ground state. The point to note is the region of agreement with the experimental data for the two different curves.

The final result we present concerns the makeup of the full photodisintegration amplitude. Barbour and Phillips have already pointed out that treating the nucleon-deuteron continuum state exactly, as

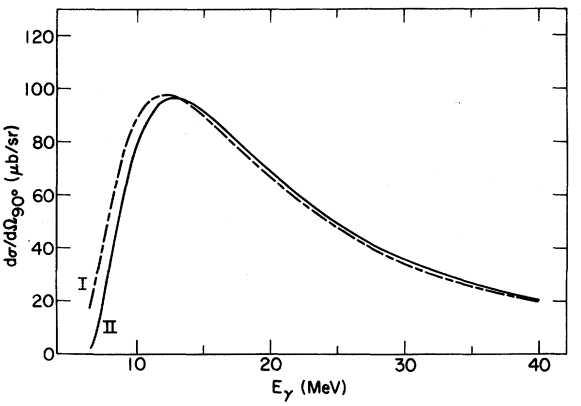

FIG. 4. Two-body 90° photodisintegration cross sections for (I) ^{3}He and (II) ^{3}H obtained with the same charge-dependent final-state parameters as in curves III and IV of Fig. 3 along with the ^{3}He and ^{3}H charge-dependent (adjusted) wave functions.

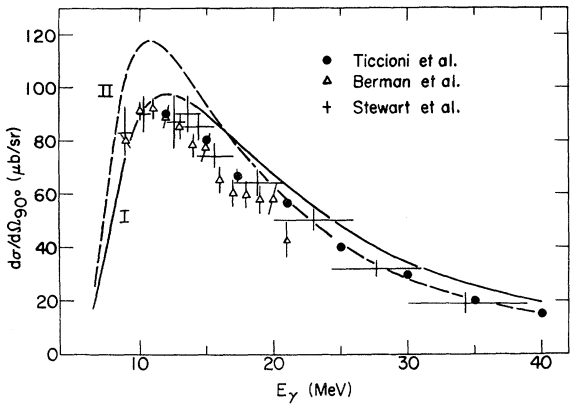

FIG. 5. Comparison of fully charge-dependent calculation (curve I, Fig. 4) and the Barbour-Phillips calculation (curve I, Fig. 3) with the available 90° ^{3}He$(\gamma, d)p$ data. The data are from (●) Ticcioni *et al.*, Ref. 11, (△) Berman *et al.*, Ref. 4, and (+) Stewart *et al.*, Ref. 3.

we have done throughout, leads to an increase at the peak in the predicted cross section of ~25% compared to neglecting the interaction between the nucleon and deuteron or using the experimental nucleon-deuteron phase shifts to represent this interaction. This raises the question of what mechanism is responsible for this enhancement. One attribute of our method for dealing with the photodisintegration amplitude, Eq. (46), is the ease with which we can handle this question. Utilizing the fact that τ_t in Eq. (46) has a pole representing the deuteron bound state, we break $M_2^t(3p^2/4M - \gamma^2/M, \vec{p})$ into its basic parts:

$$M_2^t = \hat{\epsilon}\cdot\hat{p}\left\{\left[1 + i\frac{8\pi^2 N_2^2}{3} p X_{tt}^1\left(p, p; \frac{3p^2}{4M} - \frac{\gamma^2}{M}\right)\right] \times \mathcal{B}_t\left(p, \frac{3p^2}{4M} - \frac{\gamma^2}{M}\right) + \text{off-shell triplet} + \text{singlet term}\right\}. \quad (55)$$

The first term represents the "Born" amplitude, i.e., no interaction between the nucleon and deuteron in the final state, and the second term is the correction to this due to the on-shell p-wave nucleon-deuteron rescattering. The third and fourth terms represent *off-shell* contributions to the nucleon-deuteron rescattering. In Table III, we list the contributions of these various pieces of the amplitude as a function of incident γ-ray energy. The values given are for the ^{3}He ground state of Barbour and Phillips with the parameters mentioned in the second paragraph of this section.

V. DISCUSSION

The four main aspects of comparing ^{3}He and ^{3}H two-body photodisintegration are the different thresholds, the different binding energies, the effect of charge-dependent nuclear interactions, and the effect of the Coulomb interaction in the ^{3}He case. When the ^{3}He and ^{3}H ground-state wave functions are identical, completely spatially symmetric $^2S_{1/2}$ forms (symmetric Tabakin in Table II) and the two-nucleon interactions in the final state are charge independent, the effect of requiring different thresholds is apparent. In Fig. 2, curve II for ^{3}H peaks ~1 MeV later and ~5% higher than for ^{3}He, curve I. This remains the case when the three-nucleon bound states are identical, but obtained by dropping the mixed-symmetric S component (Tabakin in Table II). The small difference between the symmetric Tabakin, curve I, and the Tabakin, curve III, is mainly attributable to their different binding energies, but indicates that the completely symmetric Tabakin wave function is a good approximation to the symmetric part of the Tabakin wave function. When the ground-state wave functions are designed to have the experimental binding energies and to predict the experimental charge radii,[25] the relative location with respect to excitation energy of the cross-section peaks remains the same, but the ^{3}He cross section now peaks ~6% higher than ^{3}H. This effect, depicted by

TABLE III. Contributions to two-body photodisintegration amplitude (fm^5) [the over-all factor eMN_2 has been removed from the amplitudes, see Eqs. (42) and (46)].

E_γ (MeV)	Born	On-shell triplet	Off-shell triplet	Off-shell singlet	Born plus on-shell triplet	Full amplitude
8	$i2.711$	$+0.218 - i0.025$	$+0.009 - i0.037$	$+0.029 + i0.490$	$+0.218 + i2.686$	$+0.256 + i3.139$
10	$i2.403$	$-0.066 - i0.159$	$-0.305 + i0.018$	$-0.416 + i0.696$	$-0.066 + i2.244$	$-0.177 + i2.960$
12	$i2.047$	$-0.197 - i0.275$	$-0.511 + i0.167$	$-0.691 + i0.494$	$-0.197 + i1.772$	$-0.377 + i2.433$
15	$i1.610$	$-0.259 - i0.331$	$-0.595 + i0.318$	$-0.760 + i0.180$	$-0.259 + i1.279$	$-0.424 + i1.777$
20	$i1.122$	$-0.254 - i0.280$	$-0.536 + i0.356$	$-0.614 - i0.078$	$-0.254 + i0.842$	$-0.332 + i1.120$
25	$i0.821$	$-0.206 - i0.208$	$-0.411 + i0.319$	$-0.449 - i0.174$	$-0.206 + i0.613$	$-0.244 + i0.758$
30	$i0.623$	$-0.158 - i0.153$	$-0.316 + i0.256$	$-0.329 - i0.180$	$-0.158 + i0.470$	$-0.171 + i0.546$
35	$i0.486$	$-0.130 - i0.115$	$-0.259 + i0.222$	$-0.258 - i0.180$	$-0.130 + i0.371$	$-0.129 + i0.413$

curves I and II in Fig. 3, is related to the smaller binding energy and larger charge radius of ^{3}He compared to ^{3}H. Charge-dependent two-nucleon interactions in the final state, which include approximately the Coulomb part of the p-p interaction, do not alter this result as can be seen by comparing curves III and IV of Fig. 3. Their effect is to push both the ^{3}He and ^{3}H cross-section peaks to a slightly higher excitation energy. With both the initial and final states obtained from charge-dependent two-nucleon interactions, the differences between the ^{3}He and ^{3}H cross-section predictions largely disappear. The two curves in Fig. 4 are almost identical, being only displaced with respect to each other at low energy due to the different thresholds. Therefore, we do not predict measurable differences between the 90° two-body photodisintegration cross sections for ^{3}H and ^{3}He.

One might argue that the above prediction loses some validity due to our representation of the p-p interaction by the low-energy (Coulomb uncorrected) p-p scattering. Moreover, compared to the Hendry-Phillips[14] approximation for including Coulomb effects in just the final state, we predict only a 1% reduction in the cross section at the peak (compare curves I and III of Fig. 3) to their 7% reduction. Certainly, an error is made with our approach, but the results of Gibson and Stephenson[19] indicate that it is not large. It emphasizes the need for developing within the Faddeev formalism a reliable method for including Coulomb interactions.

In Fig. 5, comparison of our charge-dependent calculation (^{3}He curve of Fig. 4) and the Barbour-Phillips result (curve I of Fig. 3) with the available 90° two-body photodisintegration data indicates favorable agreement with the former. The Barbour-Phillips curve peaks at ~118 μb/sr and the charge-dependent result at ~95 μb/sr, whereas the experimental data cluster at a value somewhat less than 90 μb/sr. Beyond $E_\gamma = 20$ MeV, the Barbour-Phillips curve agrees with the data. In contrast, the charge-dependent calculation peaks somewhat above the data and tends to remain slightly above the data in the region from 15 to 40 MeV. We conjecture that proper inclusion of the tensor force in our triplet interaction, for both the initial and final states, would lower our results, as it did in Hendry and Phillips,[14] and lead to better agreement with the 90° data.

Why do we obtain a lower value for the peak cross section than Barbour, Phillips, and Hendry? Clearly, from the above discussion, the answer lies wholely within the ground-state wave function, since the charge-dependent effects in the final state are small. The ground-state wave functions are essentially identical except for the spectator functions. The Barbour-Phillips spectator functions fall off more rapidly in momentum space than the ones obtained from solving Schrödinger's equation (see Table II). This means the Barbour-Phillips ground-state wave functions contain more low-momentum components, or equivalently, place more emphasis on the asymptotic coordinate-space region; whereas, our spectator functions contain more intermediate momentum components and thus emphasize the asymptotic coordinate-space region less. In fact, we were unable to obtain a good fit to our numerical tabulations of the spectator functions with a single-parameter double-pole form like that of Barbour and Phillips.[26]

The strong emphasis on the asymptotic region by Barbour and Phillips arises from their determination of the spectator function parameter by the trinucleon charge radii. This emphasis manifests itself in the large values of C^2 obtained for their wave functions: $C^2(^3\mathrm{H}) = 3.84$ and $C^2(^3\mathrm{He}) = 3.26$. Our charge-dependent (adjusted) wave functions yield[27] $C^2(^3\mathrm{H}) = 2.58$ and $C^2(^3\mathrm{He}) = 2.39$ with the charge radius of ^{3}H predicted to be 1.74 fm and that of ^{3}He to be 1.77 fm, which are within the uncertainty of the symmetric average of the experimental radii (see Table II).[25] The point is that separable-model three-body wave functions can be obtained which do not give values of C^2 greater than those obtained from dispersion-theory methods, while remaining compatible with the charge radii. Dispersion methods yield $C^2(^3\mathrm{H})$ values as follows: (1) forward dispersion relations (nd)[28]—2.4 ± 0.4; (2) partial-wave dispersion relations[29]—2.6 ± 0.4 and 3.4; and (3) conformal-mapping method[30]—~2.8. Kim and Tubis[31] predict $C^2(^3\mathrm{H}) = 2.86 \pm 0.03$ with a triton wave function obtained from the Reid soft-core potential which predicts that the binding energy of ^{3}H is 6.70 MeV. $C^2(^3\mathrm{He})$ is more elusive due to the additional complication of the Coulomb interaction, but the value of $C^2(^3\mathrm{He}) = 2.88$ obtained by Kisslinger[32] with the conformal-mapping method applied to n-^{3}He scattering is probably the most reliable. Clearly, our predicted values of C^2 are consistent with values extracted from the experimental data, whereas those of Barbour and Phillips are considerably larger. This correlates closely with the difference in the peak values of the 90° cross sections.[33]

The last point we discuss concerns the mechanism responsible for the ~25% enhancement at the peak of the 90° cross section due to final-state rescattering. Table III clearly indicates that including only the on-shell nucleon-deuteron rescattering does not enhance the cross section, but actually decreases it ~10%. Adding the off-shell triplet does not make a significant difference either. The enhancement arises solely from the off-shell singlet rescattering piece. Pictorially, this piece cor-

responds to the three-body nucleus absorbing an $E1$ photon, then disintegrating into a propagating intermediate state composed of a singlet correlated-pair plus nucleon which rescatter and emerge as an on-shell nucleon plus deuteron state. The large magnitude of this amplitude compared to the off-shell triplet can be understood by comparing the X_{ts} and X_{tt} equations, Eqs. (48)–(51). Note that $C_{ts}=-3C_{tt}$. This leads to $\mathrm{Re}X_{ts}\approx -4\,\mathrm{Re}X_{tt}$ and $|\,\mathrm{Im}X_{ts}\,|\approx|\,\mathrm{Im}X_{tt}\,|\approx\frac{1}{4}|\,\mathrm{Re}X_{ts}\,|$ in the region where the major contribution to the integral terms in Eq. (46) occurs, which combined with $\mathcal{B}_t \lesssim \mathcal{B}_s$ and $\tau_t \sim \tau_s$, leads to the dominance of the singlet rescattering effects when compared with the triplet rescattering effects.

VI. CONCLUSIONS

In summary, the main conclusions from the previous section are as follows:
(1) The ^{3}He and ^{3}H 90° photodisintegration cross sections are essentially identical in shape, only displaced ~1 MeV with respect to each other due to the different thresholds, when both initial and final states are treated consistently.
(2) The peak value of the $^3\mathrm{He}(\gamma, d)p$ 90° differential cross section is predicted to be ~95 μb/sr.
(3) Predictions for the $^3\mathrm{He}(\gamma, d)p$ cross section and the square of the asymptotic normalization constant for the nucleon-deuteron tail in the ground-state three-nucleon wave function are sensitive to the form of the spectator functions in the ground-state wave functions based on separable potentials.
(4) The dominant mechanism contributing to the final-state enhancement at the peak of the $^3\mathrm{He}(\gamma, d)p$ cross section is the $E1$ absorption of a photon by ^{3}He, disintegration into an intermediate state composed of a nucleon plus singlet correlated pair, and subsequent rescattering to emerge as an on-shell proton plus deuteron.

ACKNOWLEDGMENTS

One of the authors (DRL) wishes to thank the George Washington University Committee on Research for a summer research grant from National Science Foundation Institutional Grant No. GU3287. Part of the computer time for this work was provided by the George Washington University computer center.

APPENDIX A: NUMERICAL METHODS

We numerically solved the coupled integral equations, Eq. (48), for the half-off-shell nucleon-correlated-pair amplitudes using standard contour-rotation techniques.[34] The variables p' and p'' are rotated from the real axis into the fourth quadrant: $p' \to p' e^{-i\Phi}$ and $p'' \to p'' e^{-i\Phi}$. The rotation angle Φ is limited by the singularity in the inhomogeneous term, $Z^1_{nn'}(p,p';3p^2/4M-\gamma^2/M)$, coming from the energy denominator $p^2+p'^2+pp'x-z=0$. To avoid this singularity, the rotation angle must be chosen such that

$$\Phi < \tan^{-1}\frac{2\gamma}{p}\,. \tag{A1}$$

Having obtained the amplitudes $X^1_{tn'}(p,p'e^{-i\Phi};3p^2/4M-\gamma^2/M)$, we compute the amplitude $M^t_2(3p^2/4M-\gamma^2/M,\vec{p})$ from them by rotating the p' integration in the second term on the right-hand side of Eq. (46). This is convenient since the bound-state pole of τ_t is avoided. However, this rotation is possible only if no singularities of τ_n or $\mathcal{B}_n$ interfere. It is easy to show that this is the case for τ_n; moreover, that fact is used in solving Eq. (48). However, the $\mathcal{B}_n$ are more complicated. Using the fact that the spectator functions, i.e., the $u(p)$ in Eq. (53b), can be fitted very accurately with analytic forms of the type

$$(1+\bar{\alpha}p^2+\bar{\beta}p^4+\bar{\gamma}p^6+\bar{\delta}p^8)^{-1},$$

we break $\mathcal{B}_n$ into a sum of two types of terms: those that require only a k integration ($k=|\vec{k}|$) and those that require both a k integration and an angular integration [see Eq. (42)]. Assuming $p' \to p' e^{-i\Phi}$, we found that if the k integration in those terms which do not involve the angular integration are rotated 45°, i.e., $k \to k e^{-i\pi/4}$, no singularities are encountered, and the singularities in the angular-integration terms are avoided by rotating k the same as p', i.e., $k \to k e^{-i\Phi}$. The p' rotation is predicated on the fact that there is no contribution from the circular arc at infinity. For the integral in Eq. (46), this can easily be shown to be the case.

Gaussian and Gegenbauer[35] quadratures were used to do the angular and momentum integrations, respectively. Care was taken to check the sensitivity to the contour rotation angle and the number of integration points. With Φ chosen to be half its maximum allowable value, we estimate our numerical error to be less than 2%.

APPENDIX B: RELATIONSHIP OF R AND C^2

Near the triton pole, the n-d center-of-mass scattering amplitude is dominated by a single term:

$$f_{nd} \approx -2\pi^2\left(\frac{4M}{3}\right)^2 \frac{|\langle\, n\,d;\vec{q}, m_d m_n|\, V_{12}\,|\,{}^3\mathrm{H}\,\rangle|^2}{q^2+4MB_2/3}\,, \tag{B1}$$

where V_{12} is the neutron-neutron interaction, $\langle n\,d;\vec{q}, m_d m_n|$ is the antisymmetrized plane-wave state describing the relative motion of neutron

(spin projection m_n) and deuteron (spin projection m_d) with momentum $\vec{q}$, and B_2 is the binding energy of the neutron and deuteron to form the triton. From this expression, we define the residue (c.m.) at the triton pole as

$$R = -\left(\frac{4M}{3}\right)^2 2\pi^2 \times [\,|\langle n\,d;\vec{q}, m_d m_n|\, V_{12}\,|\,^3\mathrm{H}\rangle\,|^2_{\text{spinav}}]_{q^2=-4MB_2/3}\,. \tag{B2}$$

The amplitude in Eqs. (B1) and (B2) can be written as

$$\langle n\,d;\vec{q}, m_d m_n|\, V_{12}\,|\,^3\mathrm{H}\rangle = -\sqrt{\tfrac{3}{2}}\,\delta_{m_f m_i}\left(\frac{3q^2}{4M}+B_2\right)\langle n\,d;\vec{q}\,|\,^3\mathrm{H}\rangle \tag{B3}$$

by use of Schrödinger's equation. The overlap integral in momentum space is

$$\langle n\,d;\vec{q}\,|\,^3\mathrm{H}\rangle = \int d^3k\,\Phi_d(k)\Psi_0^s(\vec{k},\vec{q})\,. \tag{B4}$$

From Eqs. (B2)–(B4), Eqs. (53) for ^{3}H, and the integral equations which the spectator functions $u(p)$ satisfy (see Gibson and Stephenson[19]), we can derive an expression for the evaluation of R. The point to note from the integral equations is that $u^t_{np}(q)$ has a pole at $q^2=-4MB_2/3$. In the limit $q^2\to -4MB_2/3$, we obtain

$$R = -\left(\frac{4\pi^2 N_3 N_2}{\sqrt{3}}\right)^2 \times\left|\int_0^\infty p^2dp\,[I_{tt}(i\mu,p)u^t_{np}(p)+I_{ts}(i\mu,p)u^s_{np}(p) +2I_{tn}(i\mu,p)u_{nn}(p)]\right|^2, \tag{B5}$$

where $\mu=(4MB_2/3)^{1/2}$. It can be shown that the quantity within the absolute-value bars is a real number.

A quantity directly relatable to R is the asymptotic normalization constant for the neutron-deuteron tail in the ^{3}H wave function denoted by the letter C. It is defined as

$$\Psi_0^s(\vec{r},\vec{\rho})\xrightarrow[|\vec{\rho}|\to\infty]{} C\left(\frac{\mu}{2\pi}\right)^{1/2}\frac{e^{-\mu\rho}}{\rho}\,\Phi_d(r)\frac{1}{\sqrt{2}}\,\chi''\eta'\,, \tag{B6}$$

where $\Phi_d(r)$ is the normalized coordinate-space deuteron wave function. After Fourier transforming the momentum-space three-body wave function to coordinate space, we take the $|\vec{\rho}|\to\infty$ limit and extract the asymptotic behavior described by Eq. (B6). We then obtain

$$C^2 = |R|/3\mu\,. \tag{B7}$$

---

†Work supported in part by the U.S. Atomic Energy Commission.

[1] I. M. Barbour and A. C. Phillips, Phys. Rev. Lett. 19, 1388 (1967); Phys. Rev. C 1, 165 (1970). References to earlier theoretical and experimental work on low-energy photodisintegration of ^{3}He can be found in these references.

[2] V. N. Fetisov, A. N. Gorbunov, and V. T. Varfolomeev, Nucl. Phys. 71, 305 (1965).

[3] J. R. Stewart, R. C. Morrison, and J. S. O'Connell, Phys. Rev. 138, B372 (1965).

[4] B. L. Berman, L. J. Koester, and J. H. Smith, Phys. Rev. 133, B117 (1964).

[5] A. van der Woude, M. L. Halbert, C. R. Bingham, and B. D. Belt, Phys. Rev. Lett. 26, 909 (1971).

[6] C. C. Chang, E. M. Diener, and E. Ventura, Phys. Rev. Lett. 29, 307 (1972); in *Proceedings of the International Conference on Few-Particle Problems in the Nuclear Interactions, Los Angeles, California, 1972* edited by I. Šlaus, S. A. Moskowski, R. P. Haddock, and W. T. H. van Oers (North-Holland, Amsterdam, 1973), p. 525.

[7] M. L. Halbert, P. Paul, K. A. Snover, and E. K. Warburton, in *Proceedings of the International Conference on Few-Particle Problems in the Nuclear Interaction, Los Angeles, California, 1972* (see Ref. 6), p. 531.

[8] D. M. Skopik and Y. M. Shin, Can. J. Phys. 50, 392 (1972).

[9] S. K. Kundu, Y. M. Shin, and G. D. Wait, Nucl. Phys. A171, 384 (1971).

[10] C. C. Chang, W. R. Dodge, and J. J. Murphy, II, Phys. Rev. C 9, 1300 (1974).

[11] G. Ticcioni, S. N. Gardiner, J. L. Matthews, and R. O. Owens, Phys. Lett. 46B, 369 (1973).

[12] J. L. Matthews, T. Kruse, M. E. Williams, R. O. Owens, and W. Savin, Nucl. Phys. A223, 221 (1974).

[13] I. M. Barbour and J. A. Hendry, Phys. Lett. 38B, 151 (1972).

[14] J. A. Hendry and A. C. Phillips, Nucl. Phys. A211, 533 (1973).

[15] A. C. Phillips, Nucl. Phys. A184, 337 (1972).

[16] M. P. Locher, Nucl. Phys. B23, 116 (1970).

[17] E. O. Alt, P. Grassberger, and W. Sandhas, Nucl. Phys. B2, 167 (1967).

[18] B. F. Gibson, in *Proceedings of the International Conference on Photonuclear Reactions and Applications, Asilomar, 1973* (U.S. Atomic Energy Commission Office of Information Service, Oak Ridge, Tennessee, 1973), p. 373.

[19] B. F. Gibson and G. J. Stephenson, Jr., Phys. Rev. C 8, 1222 (1973).

[20] The reader is reminded that by taking only the spatially

symmetric part of the ^{3}He or ^{3}H ground-state wave function, when the interactions are both spin *and* charge dependent, means that not only an $I=\frac{1}{2}$ spatially mixed-symmetric part has been dropped, but also an $I=\frac{3}{2}$ spatially mixed-symmetric part.

[21]A. G. Sitenko and V. F. Kharchenko, Nucl. Phys. 49, 15 (1963).

[22]The scattering lengths and effective ranges given in Table I are from the following references: triplet I, R. Wilson, *Neutron Standards and Flux Normalization, AEC Symposium Series 23* (Argonne National Laboratory, Argonne, 1970), pp. 27–41, CONF-701002; triplet III, Barbour and Phillips, Ref. 1.; triplet II and singlet II, F. Tabakin, Phys. Rev. 137, B75 (1965); all the remaining singlets, E. M. Henley and D. H. Wilkinson, in *Proceedings of the International Conference on Few-Particle Problems in the Nuclear Interaction, Los Angeles, California, 1972* (see Ref. 6), pp. 229–233, 242–243; H. P. Noyes, Annu. Rev. Nucl. Sci. 22, 465 (1972); H. P. Noyes and H. M. Lipinski, Phys. Rev. C 4, 995 (1972); and E. M. Henley, in *Isospin in Nuclear Physics*, edited by D. H. Wilkinson (North-Holland, Amsterdam, 1969).

[23]Though we have parametrized their spectator functions with our form const./$(1+\bar{\alpha}p^2+\bar{\beta}p^4+\bar{\gamma}p^6)$, it should be emphasized that their spectator functions are *one-parameter* double-pole forms. With the three-body binding energy set to the experimental value, their single parameter is adjusted to give the experimental three-body charge radius.

[24]See also B. F. Gibson and D. R. Lehman, in *Proceedings of the International Conference on Photonuclear Reactions and Applications, Asilomar, 1973* (See Ref. 18), p. 505.

[25]H. Collard, R. Hofstadter, E. B. Hughes, A. Johansson, M. R. Yearian, R. B. Day, and R. T. Wagner, Phys. Rev. 138, B57 (1965); J. S. McCarthy, I. Sick, R. R. Whitney, and M. R. Yearian, Phys. Rev. Lett. 25, 884 (1970).

[26]The effect of arbitrarily adjusting the binding energy to the experimental value, the remainder of the wave function unchanged, can be seen by comparing curves III and IV of Fig. 2. Barbour and Phillips went one step further by adjusting the spectator function to fit the rms charge radius.

[27]C^2 values are computed directly from parameters in Table II, i.e., N_2 must be adjusted to account for the slight change in λ for the triplet n-p interaction.

[28]M. P. Locher, Nucl. Phys. B23, 116 (1970).

[29]L. P. Kok and A. S. Rinat, Nucl. Phys. A156, 593 (1970); R. Bower, Ann. Phys. (N.Y.) 73, 372 (1972).

[30]S. Dubnicka, O. V. Dumbrais, and F. Nichitiu, Nucl. Phys. A217, 535 (1973).

[31]Y. E. Kim and A. Tubis, Phys. Rev. Lett. 29, 1017 (1972).

[32]L. S. Kisslinger, Phys. Lett. 47B, 93 (1973).

[33]Extraction of $C^2(^3\mathrm{He})$ by Lim from the work of Knight, O'Connell, and Prats on $\gamma+{}^3\mathrm{He}\rightarrow p+d$ does not appear justified on two grounds: (1) Final-state p-d rescattering has been neglected, and (2) the effect of neglecting the (2,31) and (3,12) terms in the symmetric ground-state wave function is not clear. See T. K. Lim, Phys. Rev. Lett. 30, 709 (1973); J. M. Knight, J. S. O'Connell, and F. Prats, Phys. Rev. 164, 1354 (1967).

[34]J. H. Hetherington and L. M. Schick, Phys. Rev. 137, B935 (1965); 156, 1647 (1967). In D. D. Brayshaw, Phys. Rev. 176, 1855 (1968), the singularity structure of the amplitudes $X^J_{nn'}(p, p'; z)$ is studied in detail.

[35]T. Brady, M. Fuda, E. Harms, J. S. Levinger, and R. Stagat, Phys. Rev. 186, 1069 (1969).